CrossMark
click for updates

North-Seeking Magnetotactic Gammaproteobacteria in the Southern Hemisphere

Pedro Leão,[a] Lia C. R. S. Teixeira,[a] Jefferson Cypriano,[a] Marcos Farina,[b] Fernanda Abreu,[a] Dennis A. Bazylinski,[c] Ulysses Lins[a]

Instituto de Microbiologia Paulo de Góes, Universidade Federal do Rio de Janeiro, Rio de Janeiro, Brazil[a]; Instituto de Ciências Biomédicas, Universidade Federal do Rio de Janeiro, Rio de Janeiro, Brazil[b]; School of Life Sciences, University of Nevada at Las Vegas, Las Vegas, Nevada, USA[c]

ABSTRACT

Magnetotactic bacteria (MTB) comprise a phylogenetically diverse group of prokaryotes capable of orienting and navigating along magnetic field lines. Under oxic conditions, MTB in natural environments in the Northern Hemisphere generally display north-seeking (NS) polarity, swimming parallel to the Earth's magnetic field lines, while those in the Southern Hemisphere generally swim antiparallel to magnetic field lines (south-seeking [SS] polarity). Here, we report a population of an uncultured, monotrichously flagellated, and vibrioid MTB collected from a brackish lagoon in Brazil in the Southern Hemisphere that consistently exhibits NS polarity. Cells of this organism were mainly located below the oxic-anoxic interface (OAI), suggesting it is capable of some type of anaerobic metabolism. Magnetosome crystalline habit and composition were consistent with elongated prismatic magnetite (Fe_3O_4) particles. Phylogenetic analysis based on 16S rRNA gene sequencing indicated that this organism belongs to a distinct clade of the *Gammaproteobacteria* class. The presence of NS MTB in the Southern Hemisphere and the previously reported finding of SS MTB in the Northern Hemisphere reinforce the idea that magnetotaxis is more complex than we currently understand and may be modulated by factors other than O_2 concentration and redox gradients in sediments and water columns.

IMPORTANCE

Magnetotaxis is a navigational mechanism used by magnetotactic bacteria to move along geomagnetic field lines and find an optimal position in chemically stratified sediments. For that, magnetotactic bacteria swim parallel to the geomagnetic field lines under oxic conditions in the Northern Hemisphere, whereas those in the Southern Hemisphere swim antiparallel to magnetic field lines. A population of uncultured vibrioid magnetotactic bacteria was discovered in a brackish lagoon in the Southern Hemisphere that consistently swim northward, i.e., the opposite of the overwhelming majority of other Southern Hemisphere magnetotactic bacteria. This finding supports the idea that magnetotaxis is more complex than previously thought.

Magnetotactic bacteria (MTB) comprise a phylogenetically and morphologically diverse group of Gram-negative aquatic bacteria ubiquitous in both freshwater and marine environments [1]. MTB biomineralize intracellular organelles called magnetosomes, consisting of a nanometer-sized single magnetic domain crystal of magnetite (Fe_3O_4) or greigite (Fe_3S_4) enveloped by a lipid bilayer membrane containing specific proteins involved in the biomineralization process [2]. Magnetosomes are usually arranged as a single or multiple chains within the cell, imparting a net magnetic dipole moment to the cell body, which causes the cell to align along the Earth's or applied magnetic field lines while cells swim propelled by flagella in a behavior called magnetotaxis [3].

MTB are generally found in their highest numbers at or very close to the oxic-anoxic interface (OAI) of sediments or water columns [2]. The inclination of the geomagnetic field lines other than at the equator appears to make chemotaxis more efficient by limiting random MTB migration in vertical redox and O_2 concentration ($[O_2]$) gradients in chemically stratified sediments and water columns. The alignment of the cell along the inclined geomagnetic field lines restricts MTB to swimming mainly upward and downward in chemically stratified water columns/sediments, while chemotaxis (e.g., aerotaxis) is used to locate and maintain an optimal position in these gradients away from oxidizing conditions and where electron donors and acceptors are both available

[4, 5]. This coordination of magnetotaxis with chemotaxis and redox potential is the most accepted model to explain magnetotaxis thus far [5].

Aerotaxis was the first chemotactic behavior associated with magnetotaxis [4], where MTB tend to swim downwards under high $[O_2]$ and upwards under low $[O_2]$ [4], demonstrating that MTB have a polarity in their swimming direction [4, 6]. Polarity of MTB is defined as the preferred swimming direction of the cells under oxic conditions. In the Northern Hemisphere, most MTB swim northward parallel to the inclination of the Earth's geomagnetic field under oxidizing conditions (high $[O_2]$) and are called north-seeking (NS) MTB. In the Southern Hemisphere, under oxic conditions, most MTB have a south-seeking (SS) polarity and thus also swim downward [4]. At the geomagnetic equator, NS and SS MTB coexist in approximately

equal numbers (6). Despite the findings described above, there appears to be a minority of cells in one hemisphere that have the opposite polarity (7). In one interesting case, the majority of a population of a specific MTB in the Northern Hemisphere is SS and appears to respond to high [O_2] by swimming southward (upward) (7). However, because cells of this MTB, tentatively identified as a close relative to the sulfate-reducing bacterium *Desulforhopalus singaporensis* (*Deltaproteobacteria*), are located at the OAI of the marine basin where they were found (7), they must have a mechanism to locate and remain at the OAI, suggesting that magnetotaxis might not work the same way in all MTB.

Phylogenetically, all known MTB belong to the *Alpha-*, *Gamma-*, and *Deltaproteobacteria* classes of the *Proteobacteria* phylum (8–12), the *Nitrospira* phylum (10, 13), the candidate division *Omnitrophica* (OP3) of the *Planctomycetes-Verrucomicrobia-Chlamydiae* (PVC) superphylum (14), and possibly the candidate phylum *Latescibacteria* (15) of the *Fibrobacteres-Chlorobi-Bacteroidetes* (FCB) superphylum (16). Identified MTB of the *Gammaproteobacteria* class are limited and include two cultured strains isolated from saline lagoons in California (17) and an uncultured strain present in a freshwater pond in Japan partially characterized using culture-independent methods (11). Other putative gammaproteobacterial MTB were found in China but identified exclusively based on 16S rRNA gene sequences recovered from a magnetic enrichment of a sample; there was no confirmation that the retrieved sequences were actually from MTB (18). Here, we characterize a novel MTB belonging to the *Gammaproteobacteria* that displays unusual NS magnetotactic behavior in the Southern Hemisphere using culture-independent techniques.

MATERIALS AND METHODS

Sampling. The sampling site was the Piripiri Lagoon (22°12.461′S, 41°28.352′W) in Jurubatiba Sandbank National Park (Parque Nacional da Restinga de Jurubatiba), Rio de Janeiro state, Brazil, which is an environmentally protected sandbank area composed of 18 coastal lagoons with unique physicochemical characteristics surrounded by shrub vegetation (19). The coastal lagoons in the park have restricted communication to the sea, but large amounts of sediment inside the lagoons can originate from coastal overwashing events.

Samples of sediment and water from the lagoons were collected in December 2013, July 2014, and April 2015 in two-liter plastic bottles (ratio 2:1 [vol/vol] sediment to water). Bottles were kept at room temperature for at least 3 weeks before examining for MTB. To harvest MTB, sediment samples were deposited in a modified glass apparatus and exposed to an artificial magnetic field for 20 min, as previously described (20). The modified glass apparatus contained two opposed capillary ends to individually collect NS-MTB and SS-MTB separately at each end. MTB swimming to each one of the capillary ends (NS-MTB and SS-MTB) were harvested using a micropipette and placed in 1.5-ml polypropylene tubes.

Estimating numbers of MTB in samples. To quantify cells of MTB, a 60-ml syringe barrel with the top orifice removed with a razor blade was buried in sediment and water of the plastic storage bottles and used as a sediment core sampler. The sediment was fractionated at 0.5-cm intervals, placed in a 15-ml polypropylene tube containing 2 ml of lagoon filter-sterilized water (filtered in 0.22-μm-pore-size filters). MTB were counted by direct observation using light microscopy.

[O_2] profiles and measurements. [O_2] profiles were determined using a Unisense OX 100 O_2 microsensor attached to an MM33 micromanipulator (Unisense, Denmark). [O_2] was measured from the air-water interface to approximately 0.15 cm deep into the sediment at 100-μm intervals.

Data were recorded with the SensorTrace Pro version 3.0.2 software (Unisense).

Light and electron microscopy. MTB in drops of magnetically and non-magnetically enriched samples were observed using the hanging drop technique with a Zeiss Axio Imager microscope (Carl Zeiss, Göttingen, Germany).

For transmission electron microscopy (TEM), a drop of water with sediment containing MTB was placed on a Formvar-coated 300 mesh copper grid, which was first allowed to air dry and then imaged with a Morgagni TEM (FEI Company, Hillsboro, OR, USA) operated at 80 kV. Magnetosome and cell measurements were determined using iTEM software (Olympus Soft Imaging Solutions). Magnetosome crystal size and shape factor were calculated for 140 magnetosomes as (length + width)/2 and width/length, respectively. Statistical variance analyses were performed using GraphPad InStat version 3.0.

For high-resolution TEM (HRTEM), cells were deposited on Formvar-coated 200 mesh copper grids and imaged with a FEG-Titan TEM (FEI Company, The Netherlands) operated at 300 kV. Fast Fourier transforms (FFT) from magnification-calibrated images were obtained using Digital Micrograph software. For elemental analysis, samples were analyzed using energy-dispersive X-ray spectroscopy (EDS) in scanning transmission electron microscopy (STEM) mode to generate elemental maps of oxygen, iron, and sulfur.

16S rRNA phylogenetic characterization and fluorescence *in situ* hybridization. Phylogenetic characterization of MTB was performed by amplifying and sequencing the 16S rRNA gene of magnetically purified MTB using PCR with *Bacteria*-specific primers 27F (5′-AGAGTTTGATC MTGGCTCAG-3′) and 1492R (5′-TACGGHTACCTTGTTACGACTT-3′) (21). Each reaction mixture contained 5 μl of sample in Tris-EDTA (TE) buffer, 20 pmol of each primer, 25 μl of GoTaq G2 Green master mix (Promega, USA), and sterile water to a final volume of 50 μl. The PCR cycling conditions were 94°C for 5 min, 35 cycles of 94°C for 30 s, 50°C for 30 s, and 72°C for 45 s, and a final step of 72°C for 10 min.

PCR products were purified using the Wizard PCR purification kit (Promega, USA), cloned into pGEM-T Easy vector according to the manufacturer's instructions (Promega), and sequenced using the Macrogen sequence service (Macrogen, South Korea). The ClustalW multiple-alignment tool from BioEdit was used to align 16S rRNA sequences (22). Phylogenetic trees were constructed with MEGA 6.06 (23), using the maximum-likelihood method (24). The bootstrap value was calculated with 1,000 replicates.

Retrieved gene sequences for specific MTB were authenticated by fluorescence *in situ* hybridization (FISH). *Gammaproteobacteria* 16S rRNA gene sequences obtained from environmental samples after magnetic enrichment were used to construct two different probes for NS MTB: NS_159 probe (5′-GCGTATGCGGTATTAGCTTGAGTTTCCCCA-3′), labeled with Atto 488 fluorochrome on both ends to enhance labeling; and NS_1419 probe (5′-ACCACTTCTGGAGCAACCCACT-3′), labeled with Alexa 488 at the 5′ end. FISH was performed using 30% formamide, according to Pernthaler et al. (25). Bacterial universal probes used as controls were EUB 338, EUB 338II, and EUB 338III (26).

Accession number(s). Sequence data were deposited at NCBI under the accession no. KU382353.

RESULTS AND DISCUSSION

Light microscopy of magnetically harvested MTB revealed two major MTB morphotypes in the Piripiri lagoon samples: vibrio-shaped cells displaying NS behavior (Fig. 1A), referred to as strain NS-1, and several coccoid morphotypes that were, as expected, SS (Fig. 1B). Both types of MTB were detected deeper than 1 cm below the water-sediment interface in the anoxic region of the sediment, suggesting both have an anaerobic aspect with respect to metabolism (Fig. 1C).

Cells of SS-MTB and strain NS-1 were distributed differently along the sediment column (Fig. 1C). SS-MTB were more abun-
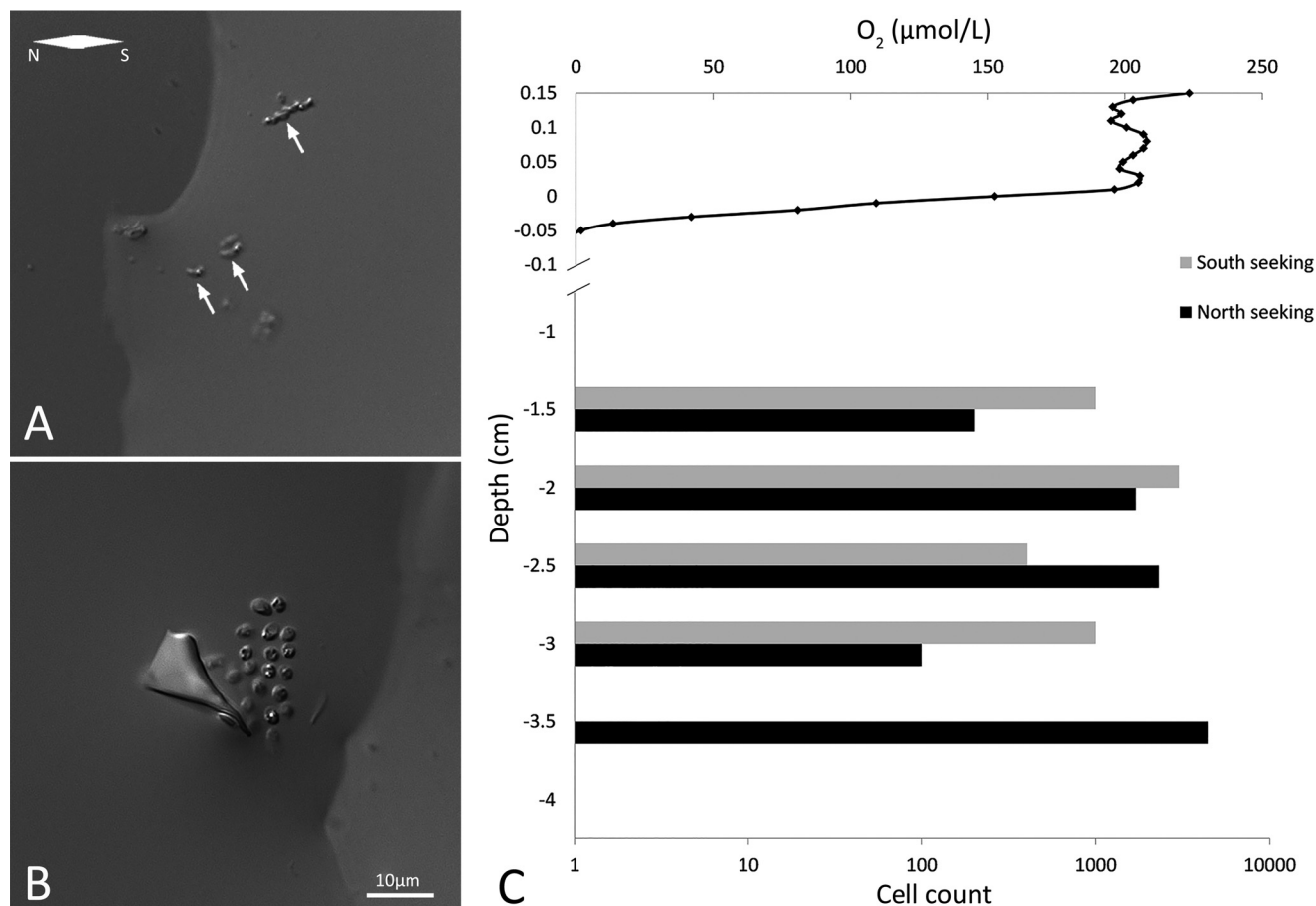
FIG 1 Cell morphologies and sediment position of MTB from Piripiri lagoon. Differential interference contrast (DIC) microscopy images show MTB at the edges of the same drop exposed to an artificial magnetic field. (A) North-seeking (NS) vibrioid cells (arrows; designated strain NS-1), which migrated to the edge of the drop adjacent to magnetic north. (B) South-seeking (SS) cocci concentrated at the drop edge adjacent to magnetic south. (C) Oxygen concentration [O_2] profile correlated with numbers of NS and SS MTB in sediment.

dant between 2 and 3 cm into the sediment but were detected deeper than 3.5 cm below the water-sediment interface. Strain NS-1 was observed in all sediment fractions, with largest number of cells between 2.5 and 3.5 cm into the sediment, deeper than the position of most SS-MTB.

To further characterize strain NS-1, we examined whole intact cells and thin sections of cells using TEM (Fig. 2). Cells were vibri-oid, averaging 2.6 ± 0.8 µm in length. Cells possessed a single flagellum at one pole of the cell (Fig. 2C). A single chain of elongated prismatic magnetosomes is aligned along the long axis of the cell (Fig. 2A and B). Various intracellular granules (Fig. 2A and B) are distributed in the cytoplasm. Electron-dense inclusions (Fig. 2A) were rarely observed and were about 43 ± 12 nm in diameter. Electron-lucent granules (Fig. 2A) were about 0.27 ± 0.10 µm in diameter and were more commonly observed in larger numbers in cells.

Ultrathin sections of cells of strain NS-1 revealed that they had a relatively typical Gram-negative cell wall, with two membrane layers clearly representing the inner cytoplasmic and outer membranes (Fig. 2C). An electron-dense layer enveloping the magnetosome crystals suggestive of a magnetosome membrane was observed (Fig. 2C). Cytoplasmic inclusions representing the intracellular granules detected in whole cells were observed in thin sections of all cells.

Magnetosome crystalline habit and composition were analyzed by TEM, HRTEM, and EDS in STEM mode. TEM and HRTEM images (Fig. 3A and E) were consistent with an elongated prismatic crystalline habit of magnetite (Fe_3O_4), as well as the fast Fourier transform (FFT) pattern of the crystalline structure determined using STEM (Fig. 3F). EDS elemental microanalysis mapping showed the presence of iron (Fig. 3G) and oxygen (Fig. 3H) but not sulfur (Fig. 3I) in magnetosome crystals, also consistent with the mineral magnetite. The bright cell granular inclusions consisted of mainly sulfur, as detected by EDS (Fig. 3F and I), and likely represent elemental sulfur globules, which have been found in other both cultured and uncultured MTB (27).

The size of the magnetosome crystals (Fig. 3B) ranged from 26.8 to 87.8 nm, with an average of 68.8 ± 16.2 nm, while the shape factor (Fig. 3C) ranged from 0.56 to 0.91 nm, with an average of 0.86 ± 0.2 nm. A scatter plot of length versus width of the magnetosome crystals from strain NS-1 is shown in Fig. 3D. The straight line corresponds to the linear regressions obtained from the data ($r = 0.96$).
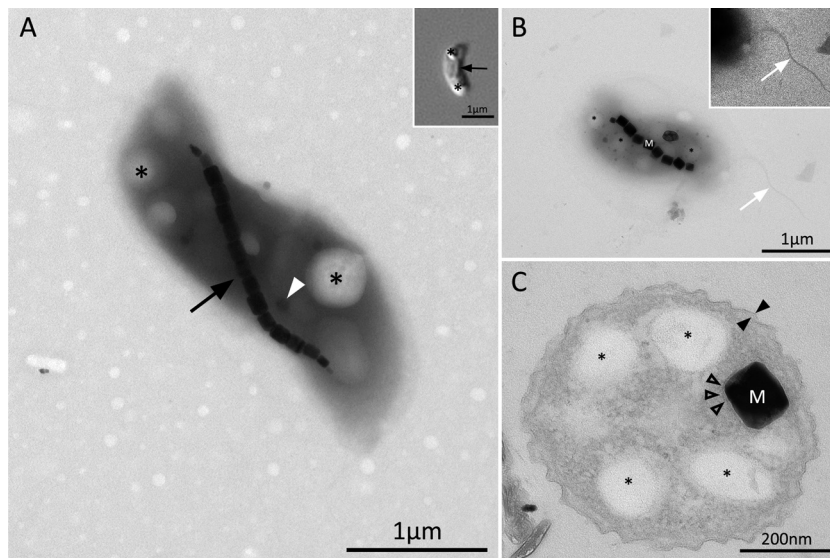
FIG 2 Ultrastructure of cells of strain NS-1. (A) Vibrioid cell showing a single magnetosome chain along the major axis of the cell (black arrow) and two intracellular granule types: electron-dense (white arrowhead) and electron-lucent (asterisks). Inset, differential interference contrast (DIC) microscopy image of a cell of strain NS-1 showing the magnetosome chain (black arrow) and intracellular granules (asterisks). (B) Transmission electron micrograph image of a cell of strain NS-1 showing the single polar flagellum (white arrows), magnetosomes (M), and intracellular granules (asterisks). Inset, high-contrast high-magnification TEM image of the polar flagellum. (C) TEM image of an ultrathin section of a stained NS-1 cell showing electron-lucent globular inclusions (asterisks) and a magnetosome (m) surrounded by an electron-dense membrane (hollow arrowheads). The cell wall structure is consistent with a trilayered Gram-negative cell wall (black arrowheads) composed of the cytoplasmic membrane and the outer membrane defining a periplasmic space.

A 16S rRNA gene was amplified, cloned, and sequenced from magnetically enriched NS-MTB. Eighteen gene sequences were recovered. Eight sequences were from *Gammaproteobacteria*, while 4 were from the *Deltaproteobacteria* class, and 6 were affiliated with phylogenetic groups not known to include MTB. The 16S rRNA gene sequences from the *Gammaproteobacteria* were ~90% similar to the gammaproteobacterial MTB strain SS-5 (accession no. HQ595729) and ~87% similar to the uncultivated magnetotactic gammaproteobacterial strain HCH5043 (accession no. JX134740) (Fig. 4).

To confirm that the gammaproteobacterial 16S rRNA sequence that we recovered was actually that of strain NS-1, two FISH probes were designed. Vibrioid NS cells (strain NS-1) clearly hybridized to the NS-1 probes (Fig. 5A to D), whereas other cells in samples did not (Fig. 5E to H), indicating that the gammaproteobacterial 16S rRNA gene sequence we recovered is that of strain NS-1.

The occurrence of a population of a single species of MTB in a coastal salt pond in the Northern Hemisphere with an opposite magnetic polarity than expected (SS in the Northern Hemisphere) was previously reported (7). This organism was nicknamed the "barbell" because the organism appeared to represent a chain of 2 to 5 (mostly 2, hence the name barbell) coccoid cells in a single structure (7). A 16S rRNA sequence was obtained from the barbell, which suggested it phylogenetically belonged to the *Deltaproteobacteria* class and was a close relative to the sulfate-reducing bacterium *Desulforhopalus singaporensis* (7), which has a similar morphology to the barbell when viewed with light microscopy. Here, we describe a population of NS MTB that appeared to consist of a single vibrioid species in sediments collected from a brackish lagoon in the Southern Hemisphere (Brazil). Both the barbell and strain NS-1 were generally present in their highest numbers in the anoxic zone of the sediment, although the barbell was also present in slightly more oxidizing areas than NS-1 (7).

Interestingly, light microscopy images of cells of the barbell and strain NS-1 are somewhat similar. Cells of strain NS-1 contain many intracellular granules/globules sometimes resembling a chain of coccoid cells (Fig. 1), similar to the morphology described for the barbell (7). The cell wall is often not obvious when prokaryotic cells contain a large number of highly refractive inclusions when viewed with differential interference contrast microscopy. There is a very strong correlation between the phylogenetic groups of MTB and the composition and morphology of their magnetosome crystals (28). All known alpha- and gammaproteobacterial MTB biomineralize cuboctahedral and elongated prismatic crystals of magnetite, while those of the *Deltaproteobacteria* synthesize bullet-shaped crystals of magnetite and/or greigite (28). Unfortunately, no electron micrographs of the barbell or their magnetosomes were provided, which might have shown that the organisms are either the same or different. Regardless, it is clear that strain NS-1 represents a new genus of MTB within the *Gammaproteobacteria*.

How can the unusual magnetotactic behavior of "opposite" polarity in MTB be explained? It has always been assumed that in natural environments, SS MTB would swim upward toward high toxic concentrations of O_2 and thus be selected against leading to the majority of MTB being NS in the Northern Hemisphere (4). The opposite would be true in the Southern Hemisphere. This model is obviously not applicable to MTB, like the barbell and NS-1. Questions raised by the unusual magnetotactic behavior of these MTB are (i) how does magnetotaxis/chemotaxis work in these organisms and (ii) is it an exclusive mechanism restricted to a small select group of MTB?
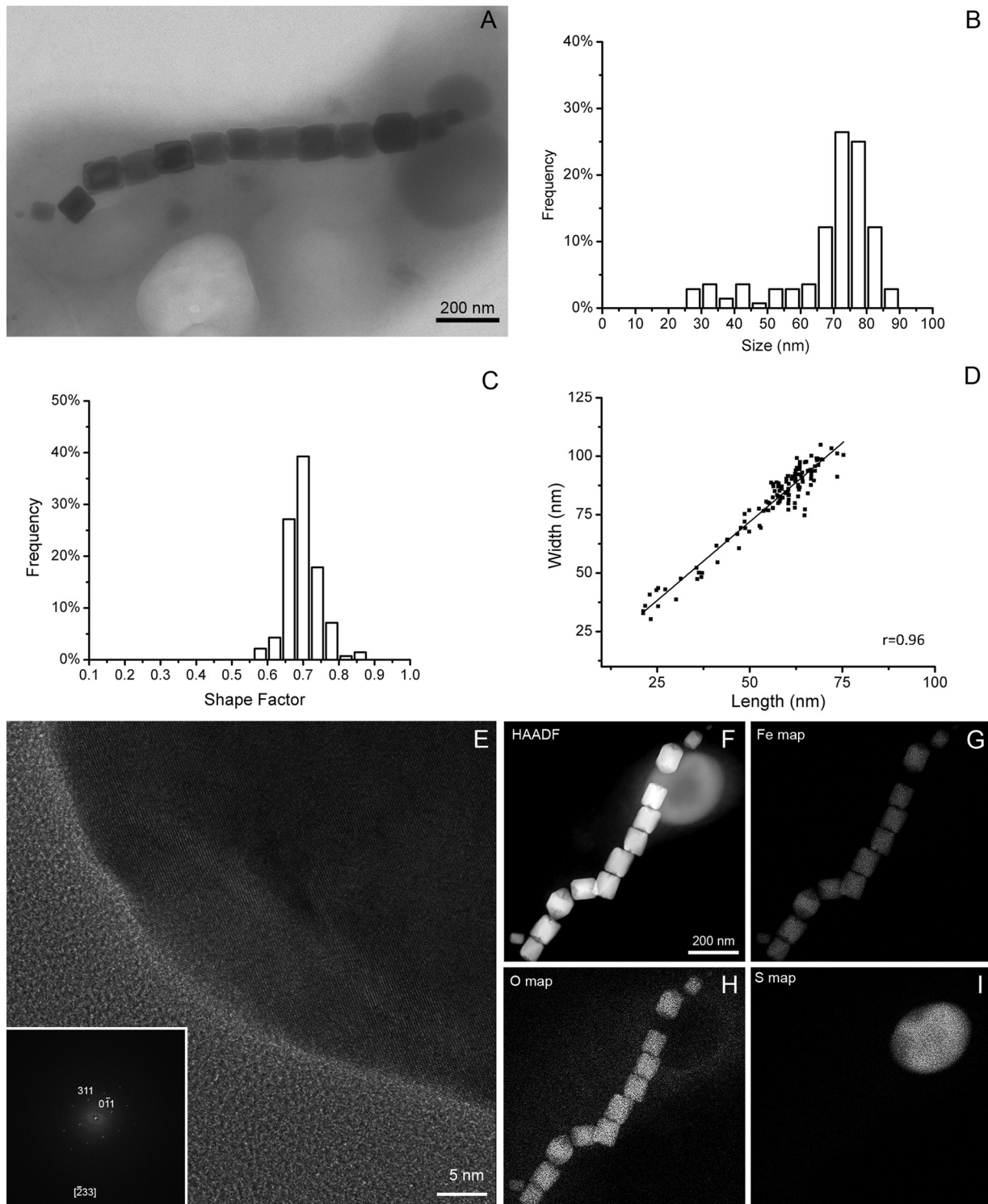
FIG 3 Magnetosomes in strain NS-1: intracellular arrangement, size distribution, and composition. (A) High-magnification TEM image of cell of NS-1 showing a single chain of elongated prismatic magnetosomes and intracellular granules (asterisks). (B and C) Size and shape factor distribution of magnetosome crystals of strain NS-1, respectively. (D) Scatter plot of magnetosome length versus width. The straight line corresponds to the linear regression obtained from the data. (E) High-resolution TEM (HRTEM) image of a single magnetosome from strain NS-1. Inset, fast Fourier transform (FFT) image corresponding to the [−233] zone axis of magnetite (Fe_3O_4). (F to I) High-angle annular dark-field (HAADF) image of a cell of NS-1 showing a chain of magnetosomes and an intracellular globule with correlating elemental maps of iron (G), oxygen (H), and sulfur (I) of the cell shown in panel F.
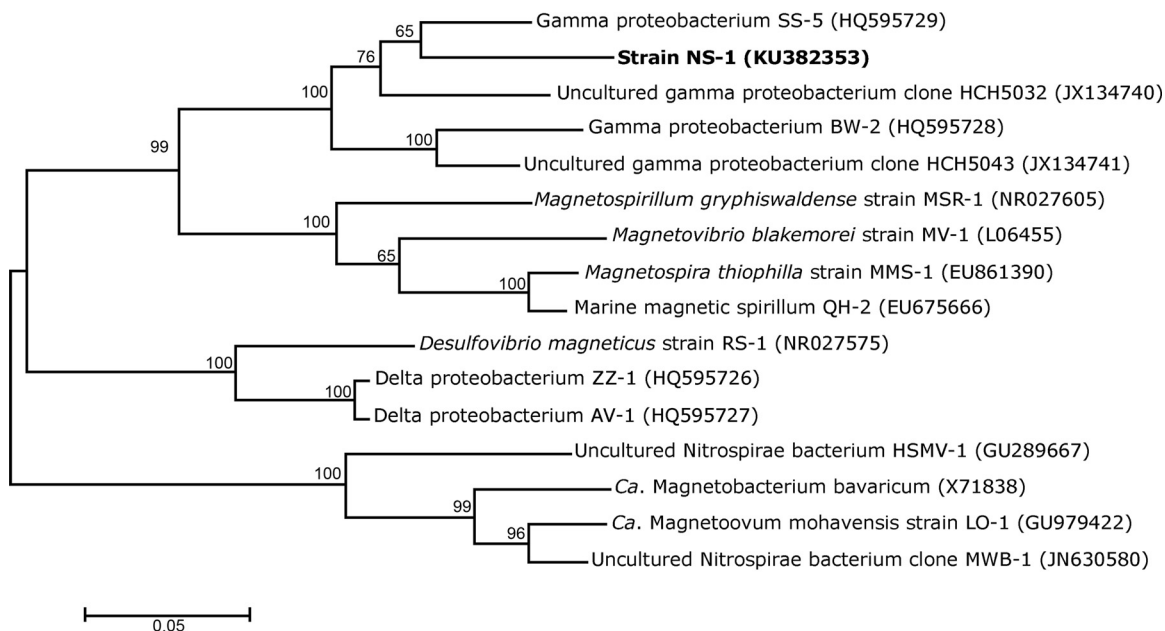
FIG 4 Phylogenetic tree based on 16S rRNA gene sequences showing the position of the strain NS-1 among other MTB of the *Gammaproteobacteria* class. Bootstrap values at nodes are percentages of 1,000 replicates. GenBank accession numbers are given in parentheses. The tree was constructed using the maximum-likelihood method algorithm.

How magnetotaxis/chemotaxis and the factors involved in controlling magnetic polarity specifically function in the barbell and in strain NS-1 is unclear. Frankel et al. (4) suggested that [O_2] is the factor that dictates the polarity of MTB, while Zhang et al. (5) reported that magnetotactic polarity was determined mainly by the oxidation/reduction potential (redox) of the environment. Unlike many magnetite-producing MTB, which are microaerophilic when respiring with O_2 and are mainly present at or very close to the OAI in natural environments (2), both the barbell and NS-1 are mainly found below the OAI in the anoxic zone, suggesting that they may be anaerobes that are not microaerophilic. This observation might also suggest that these organisms are not aerotactic. These may be key environmental factors in dictating polarity in these MTB, as well as in defining the chemical signals that control the direction of flagellar rotation. On the other hand, greigite-producing MTB are anaerobes (29) and are found in the anoxic zone (30) but still show a polarity similar to the majority of
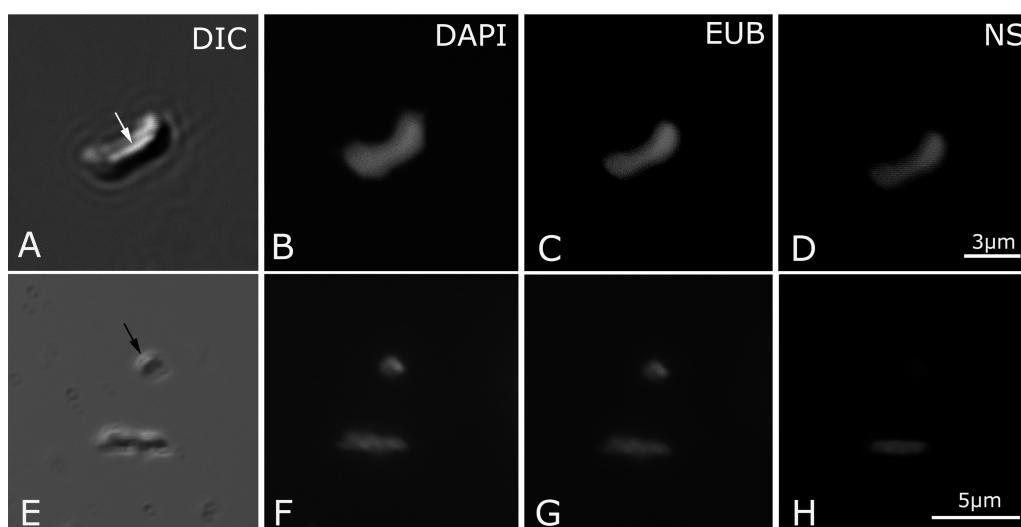

FIG 5 Fluorescent *in situ* hybridization (FISH) of strain NS-1. (A and E) High-magnification DIC images of vibrioid and coccoid (black arrow) cells. A magnetosome chain is shown in the vibrioid cell in A (white arrow). (B and F) Fluorescence microscopy images of the same cells stained with 4′,6-diamidino-2-phenylindole (DAPI). (C and G) Fluorescence microscopy images of the same cells hybridized with the *Bacteria*-specific EUB probe. (D and H) Fluorescence microscopy images of the same cells hybridized with probes specifically designed based on the 16S rRNA gene sequences obtained from strain NS-1. Note that labeling occurs only in the vibrioid cell, not in the coccus.

MTB. The fact that both the barbell and NS-1 are found at specific depths in chemically stratified habitats suggests that magnetotaxis, as in other MTB, functions as a means of locating and maintaining an optimal position in vertical chemical gradients.

Based on what is currently known, the unexpected magnetotactic behavior described in the barbell and NS-1 might represent an exclusive mechanism restricted to a small select group(s) of MTB. More studies, perhaps with pure cultures, are clearly necessary to identify the chemotactic sensors associated with magnetotaxis that should lead to an understanding how magnetotaxis functions in these unusual MTB.

REFERENCES

1. **Lin W, Bazylinski DA, Xiao T, Wu LF, Pan Y.** 2014. Life with compass: diversity and biogeography of magnetotactic bacteria. Environ Microbiol **16:**2646–2658. http://dx.doi.org/10.1111/1462-2920.12313.
2. **Lefèvre CT, Bazylinski DA.** 2013. Ecology, diversity, and evolution of magnetotactic bacteria. Microbiol Mol Biol Rev **77:**497–526. http://dx.doi.org/10.1128/MMBR.00021-13.
3. **Blakemore R.** 1975. Magnetotactic bacteria. Science **190:**377–379. http://dx.doi.org/10.1126/science.170679.
4. **Frankel RB, Bazylinski DA, Johnson MS, Taylor BL.** 1997. Magneto-aerotaxis in marine coccoid bacteria. Biophys J **73:**994–1000. http://dx.doi.org/10.1016/S0006-3495(97)78132-3.
5. **Zhang WJ, Chen C, Li Y, Song T, Wu LF.** 2010. Configuration of redox gradient determines magnetotactic polarity of the marine bacteria MO-1. Environ Microbiol Rep **2:**646–650. http://dx.doi.org/10.1111/j.1758-2229.2010.00150.x.
6. **de Araujo FF, Germano FA, Gonçalves LL, Pires MA, Frankel RB.** 1990. Magnetic polarity fractions in magnetotactic bacterial populations near the geomagnetic equator. Biophys J **58:**549–555. http://dx.doi.org/10.1016/S0006-3495(90)82398-5.
7. **Simmons SL, Bazylinski DA, Edwards KJ.** 2006. South-seeking magnetotactic bacteria in the Northern Hemisphere. Science **311:**371–374. http://dx.doi.org/10.1126/science.1122843.
8. **Bazylinski DA, Williams TJ, Lefèvre CT, Berg RJ, Zhang CL, Bowser SS, Dean AJ, Beveridge TJ.** 2013. *Magnetococcus marinus* gen. nov., sp. nov., a marine, magnetotactic bacterium that represents a novel lineage (*Magnetococcaceae* fam. nov., *Magnetococcales* ord. nov.) at the base of the *Alphaproteobacteria*. Int J Syst Evol Microbiol **63:**801–808. http://dx.doi.org/10.1099/ijs.0.038927-0.
9. **Morillo V, Abreu F, Araujo AC, de Almeida LGP, Enrich-Prast A, Farina M, Vasconcelos ATR, Bazylinski DA, Lins U.** 2014. Isolation, cultivation and genomic analysis of magnetosome biomineralization genes of a new genus of South-seeking magnetotactic cocci within the *Alphaproteobacteria*. Front Microbiol **5:**72. http://dx.doi.org/10.3389/fmicb.2014.00072.
10. **Lefèvre CT, Abreu F, Schmidt ML, Lins U, Frankel RB, Hedlund BP, Bazylinski DA.** 2010. Moderately thermophilic magnetotactic bacteria from hot springs in Nevada. Appl Environ Microbiol **76:**3740–3743. http://dx.doi.org/10.1128/AEM.03018-09.
11. **Taoka A, Kondo J, Oestreicher Z, Fukumori Y.** 2014. Characterization of uncultured giant rod-shaped magnetotactic *Gammaproteobacteria* from a freshwater pond in Kanazawa, Japan. Microbiology **160:**2226–2234. http://dx.doi.org/10.1099/mic.0.078717-0.
12. **Sakaguchi T, Arakaki A, Matsunaga T.** 2002. *Desulfovibrio magneticus* sp. nov., a novel sulfate-reducing bacterium that produces intracellular single-domain-sized magnetite particles. Int J Syst Evol Microbiol **52:**215–221. http://dx.doi.org/10.1099/00207713-52-1-215.
13. **Lin W, Jogler C, Schüler D, Pan Y.** 2011. Metagenomic analysis reveals unexpected subgenomic diversity of magnetotactic bacteria within the phylum *Nitrospirae*. Appl Environ Microbiol **77:**323–326. http://dx.doi.org/10.1128/AEM.01476-10.
14. **Kolinko S, Jogler C, Katzmann E, Wanner G, Peplies J, Schüler D.** 2012. Single-cell analysis reveals a novel uncultivated magnetotactic bacterium within the candidate division OP3. Environ Microbiol **14:**1709–1721. http://dx.doi.org/10.1111/j.1462-2920.2011.02609.x.
15. **Lin W, Pan Y.** 2015. A putative greigite-type magnetosomes gene cluster from the candidate phylum Latescibacteria. Environ Microbiol Rep **7:**237–242. http://dx.doi.org/10.1111/1758-2229.12234.
16. **Rinke C, Schwientek P, Sczyrba A, Ivanova NN, Anderson IJ, Cheng JF, Darling A, Malfatti S, Swan BK, Gies EA, Dodsworth JA, Hedlund BP, Tsiamis G, Sievert SM, Liu WT, Eisen JA, Hallam SJ, Krypides NC, Stepanauskas R, Rubin EM, Hugenholtz P, Woyke T.** 2013. Insights into the phylogeny and coding potential of microbial dark matter. Nature **499:**431–437. http://dx.doi.org/10.1038/nature12352.
17. **Lefèvre CT, Viloria N, Schmidt ML, Pósfai M, Frankel RB, Bazylinski DA.** 2012. Novel magnetite-producing magnetotactic bacteria belonging to the *Gammaproteobacteria*. ISME J **6:**440–450. http://dx.doi.org/10.1038/ismej.2011.97.
18. **Wang Y, Lin W, Li J, Pan Y.** 2013. High diversity of magnetotactic *Deltaproteobacteria* in a freshwater niche. Appl Environ Microbiol **79:**2813–2817. http://dx.doi.org/10.1128/AEM.03635-12.
19. **Esteves FA.** 1998. Ecologia das lagoas costeiras do Parque Nacional da Restinga de Jurubatiba e do Município de Macaé (RJ). Universidade Federal do Rio de Janeiro Press, Rio de Janeiro, Brazil.
20. **Lins U, Freitas F, Keim CN, Lins de Barros HGP, Esquivel DMS, Farina M.** 2003. Simple homemade apparatus for harvesting uncultured magnetotactic microorganisms. Braz J Microbiol **34:**111–116. http://dx.doi.org/10.1590/S1517-83822003000200004.
21. **Lane DJ.** 1991. 16S/23S rRNA sequencing, p 115–175. *In* Stackebrandt E, Goodfellow M (ed), Nucleic acid techniques in bacterial systematics. Wiley & Sons, Chichester, United Kingdom.
22. **Hall TA.** 1999. BioEdit: a user-friendly biological sequence alignment editor and analysis program for Windows 95/98/NY. Nucleic Acids Symp Ser (Oxf) **41:**95–98.
23. **Tamura K, Stecherv G, Peterson D, Filipski A, Kumar S.** 2013. MEGA6: Molecular Evolutionary Genetics Analysis version 6.0. Mol Biol Evol: **30:**2725–2729. http://dx.doi.org/10.1093/molbev/mst197.
24. **Saitou N, Nei M.** 1987. The neighbor-joining method: a new method for reconstructing phylogenetic trees. Mol Biol Evol **4:**406–425.
25. **Pernthaler J, Glöckner FO, Schönhuber W, Amann R.** 2001. Fluorescence *in situ* hybridization (FISH) with rRNA-targeted oligonucleotide probes. Methods Microbiol **30:**207–226. http://dx.doi.org/10.1016/S0580-9517(01)30046-6.
26. **Daims H, Brühl A, Amann R, Schleifer K-H, Wagner M.** 1999. The domain-specific probe EUB338 is insufficient for the detection of all bacteria: development and evaluation of a more comprehensive probe set. Syst Appl Microbiol **22:**434–444. http://dx.doi.org/10.1016/S0723-2020(99)80053-8.
27. **Bazylinski DA, Dean AJ, Williams TJ, Long LK, Middleton SL, Dubbels BL.** 2004. Chemolithoautotrophy in the marine, magnetotactic bacterial strains MV-1 and MV-2. Arch Microbiol **182:**373–387. http://dx.doi.org/10.1007/s00203-004-0716-y.
28. **Pósfai M, Lefèvre CT, Trubitsyn D, Bazylinski DA, Frankel RB.** 2014.

Phylogenetic significance of composition and crystal morphology of magnetosome minerals. Front Microbiol 4:344. http://dx.doi.org/10.3389/fmicb.2013.00344.

29. Abreu F, Morillo V, Nascimento FF, Werneck C, Cantão ME, Ciapina LP, de Almeida LG, Lefèvre C, Bazylinski DA, Vasconcelos AT, Lins U. 2014. Deciphering unusual uncultured magnetotactic multicellular prokaryotes through genomics. ISME J 8:1055–1068. http://dx.doi.org/10.1038/ismej.2013.203.

30. Simmons SL, Sievert SM, Frankel RB, Bazylinski DA, Edwards KJ. 2004. Spatiotemporal distribution of marine magnetotactic bacteria in a seasonally stratified coastal salt pond. Appl Environ Microbiol 70:6230–6239. http://dx.doi.org/10.1128/AEM.70.10.6230-6239.2004.